Temperature Dependence of Leakage Current in InAs Avalanche Photodiodes

Pin Jern Ker, Andrew R. J. Marshall, Andrey B. Krysa, John P. R. David, *Senior Member, IEEE*, and Chee Hing Tan, *Member, IEEE*

***Abstract*— Measurement and analysis of the temperature dependence of bulk and surface leakage currents in InAs avalanche photodiodes have been performed between 77 K and 290 K. At unity gain, SU-8 passivated InAs photodiodes have low dark current densities of 100 mA/cm^2 at 290 K and 150 nA/cm^2 at 77 K. An avalanche multiplication factor of 25 was measured at 13 V and 19.5 V at 290 K and 77 K, respectively. The photodiodes exhibit dynamic resistance-area products, calculated at 0.1 V of 34 Ω−cm^2 at 290 K and 910 MΩ−cm^2 at 77 K. Our analysis showed that between the temperatures of 200 K and 290 K, the bulk leakage current is proportional to n_i^2 whereas the surface leakage current is proportional to n_i from 77 K to 290 K, where n_i is the intrinsic carrier concentration. The activation energies deduced were 0.36 eV and 0.18 eV suggesting diffusion dominated bulk current and generation and recombination dominated surface current.**

***Index Terms*— Avalanche photodiode, impact ionization, InAs, leakage current.**

I. Introduction

INDIUM arsenide (InAs), with a bandgap $E_g = 0.36$ eV, can provide good quantum efficiency at visible to the infrared wavelengths (up to 3.5μm). There is an increasing interest in the spectral range from 1.55μm to 3.5μm because it can be utilised in active imaging [1], gas sensing [2], free space communications [3] and satellite based environmental monitoring [4]. In these applications, the photon flux can be low and amplification of the signal is necessary. However external amplification can degrade the overall signal to noise ratio especially when high gain at high frequency is required.

Avalanche photodiodes (APDs) can circumvent this problem since their internal gain mechanism can significantly improve the overall system sensitivity. For instance, HgCdTe APDs have been incorporated into focal plane arrays (FPAs) to facilitate long range high sensitivity active imaging [1]. Although the impact ionization process provides the avalanche gain, it is also a stochastic mechanism, leading to a fluctuation of gain around its mean value, typically characterised by the excess noise factor. The local model of impact ionization [5] shows that this excess noise factor is dependent on the mean gain and the ionization coefficient ratio. A large difference between the electron ionization coefficient (α) and hole ionization coefficient (β) will minimise the excess noise factor. In the ideal case of α (or β) being equal to zero, the excess noise factor approaches 2 at high gain due to the elimination of impact ionization by feedback carriers. HgCdTe APDs have demonstrated this favourable excess noise characteristic [6]. However there are several challenges preventing a mass market exploitation of HgCdTe APDs including the high production cost due to challenging growth and fabrication, as well as relatively small lattice matched CdZnTe substrates [7] . The challenges in HgCdTe device fabrication are largely associated with the weak bonding of Hg in the crystal lattice [8]. Hence HgCdTe devices are relatively more susceptible to process induced damage. These issues, coupled with the limited availability of HgCdTe APDs in the mass market, motivated research for a HgCdTe-like material.

Recently, Marshall *et al*. demonstrated that InAs APDs can provide useful avalanche multiplication, at bias voltage less than 10 V, as well as confirming an electron-only multiplication behaviour similar to that of HgCdTe APDs. This showed the potential of InAs APDs for low cost high performance HgCdTe-like APD arrays for active imaging [9]. In InAs APDs, the electron initiated multiplication excess noise factor (F_e) is <2 at high gain, corresponding to single carrier ionization [10]. Relying on the established and widely available III-V growth and processing technology, InAs APDs have a great potential for large-scale production. However, due to the narrow bandgap of InAs, InAs photodiodes exhibit higher room temperature dark current than photodiodes made from wider bandgap materials such as InGaAs. Consequently, to achieve the same dark current density as in InGaAs photodiodes, cooling is necessary. An additional challenge in InAs photodiodes is the difficulty in suppressing the surface leakage current [11]. Hence there is a need to understand the significance of both the surface and bulk leakage currents as a function of temperature.

Fabrication and dark current analysis of InAs photodiodes were previously carried out by Lin *et al*. [12], [13]. They reported that unpassivated InAs p-i-n photodetectors grown by molecular beam epitaxy (MBE) with a 720-nm thick intrinsic layer exhibit zero bias resistance-area products (R_0A) of 8.1 Ω-cm^2 and 1.3 MΩ-cm^2 at room temperature and 77 K respectively [12]. They also demonstrated that at a reverse bias

Manuscript received March 11, 2011; revised May 20, 2011; accepted May 24, 2011. Date of current version July 15, 2011. This work was supported in part by the Electro-Magnetic Remote Sensing Defense Technology Center and the Engineering and Physical Sciences Research Council, under Grant EP/H031464/1.

P. J. Ker, A. B. Krysa, J. P. R. David, and C. H. Tan are with the Department of Electronic and Electrical Engineering, University of Sheffield, Sheffield S1 3JD, U.K. (e-mail: elp09pk@sheffield.ac.uk; a.krysa@sheffield.ac.uk; j.p.david@sheffield.ac.uk; c.h.tan@sheffield.ac.uk).

A. R. J. Marshall is with the Department of Physics, Lancaster University, Lancaster LA1 4YW, U.K. (e-mail: a.r.marshall@lancaster.ac.uk).

Digital Object Identifier 10.1109/JQE.2011.2159194

of 0.5 V, the room temperature dark current density reduced from 0.83 A/cm^2 to 0.18 A/cm^2 as the i-layer increased from 0 to 720 nm [13]. The measured leakage current in a photodiode with an area of 3.14×10^{-4}cm^2 became dominated by background infrared induced photocurrent and saturated at 0.1 nA for temperatures below 80 K [13]. However, the operating voltage of the InAs photodiodes is still limited below 0.5 V. A detailed study on the dependence of surface and bulk leakage currents on high reverse bias and the dependence of these leakage current components on temperature has not been reported to date.

In this work, we report a systematic study and analysis of leakage currents in InAs APD as a function of temperature. The InAs APDs have a nominal 6μm intrinsic layer, as well as a 1.5μm n^+ and 3.5μm p^+ cladding layers. These 11-μm thick structures impose stringent requirements on the fabrication and processing of the APDs. The surface of the mesa was sufficiently passivated by SU-8 to suppress the surface leakage current and ensure bulk dominated leakage current at room temperature. The dark current analysis encompassed a wide temperature range from 77 K to 290 K. Analysis of the bulk and surface current components enables the extraction of activation energies. To obtain a desired dark current density for a specific application, the required operating voltage, operating temperature and the area of an InAs APD can also be determined from this analysis.

II. Experimental Detail, Results and Analysis

An InAs n-i-p structure was grown on a p-type doped InAs substrate using metal organic vapour phase epitaxy (MOVPE) at a growth temperature of 600 °C. The p- and n-type dopants were zinc and silicon respectively. The fabrication of circular mesa photodiodes, with 205-μm, 105-μm, 55-μm and 30-μm radii, was carried out by wet etching using a 1:1:1 mixture of phosphoric acid, hydrogen peroxide, and de-ionized water followed by a finishing etch using a 1:8:80 mixture of sulphuric acid, hydrogen peroxide, and de-ionized water [11]. The etched mesa walls were then passivated by depositing a layer of SU-8 [14]. Ti/Au (20 nm/200 nm) was deposited by metal evaporation as both the p- and n-type contacts without annealing. Due to the high room temperature leakage current at large reverse biases, the device capacitance was measured at 77 K and it confirmed that doping concentrations $>5\times10^{17}$cm^{-3} were obtained in both the n- and p-type cladding layers and an unintentional doping concentration varying between 7×10^{14}cm^{-3}and 2×10^{15}cm^{-3} was obtained in the intrinsic regions or i-layer. Depletion widths up to 4.5μm were achieved within the bias range reported.

The forward and reverse current-voltage (I-V) measurements were performed at temperatures of 77 K to 290 K using a Janis ST-500 series low temperature on-wafer probe station. At each temperature, all the 205-μm, 105-μm, 55-μm and 30-μm radii devices were tested and the data were recorded. The dark currents for photodiodes with a radius of 55μm are shown in figure 1. Clearly, the surface leakage current is sufficiently suppressed that the reverse leakage current decreases with decreasing temperature. The Ti/Au metal forms good contact with InAs photodiodes since the series resistances for all sizes of photodiodes are between 5 Ω and 12 Ω at room temperature. The ideality factor is ∼1.1, suggesting relatively good quality n-i-p junctions.

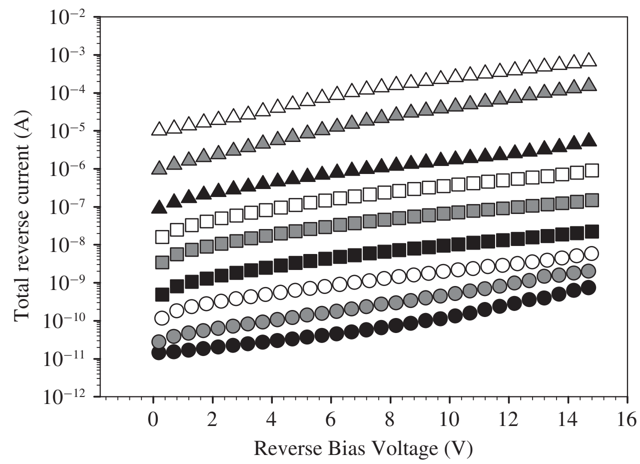

Fig. 1. Reverse dark currents for n-i-p InAs diodes with a radius of 55 μm at temperatures of 77 K (●), 100 K (●), 125 K (o), 150 K (■), 175 K (■), 200 K (□), 220 K (▲), 250 K (▲), and 290 K (△).

Another parameter which is closely related to the performance and quality of an APD is the dynamic resistance-area product $R_dA = (dV/dJ_A)$ at a specific reverse bias voltage, where V is the bias voltage, J_A is the leakage current density, R_d is the dynamic resistance and A is the area of photodiode. From 0.1 V to 15 V, the R_dA of our InAs APD was calculated to be between 34Ω-cm^2 and 0.6Ω-cm^2 at room temperature. However at 77 K, these values increased to 910 MΩ-cm^2 and 172 kΩ-cm^2.

To investigate and analyse the temperature dependence of the total leakage currents, dark currents at 0.3 V, prior to the onset of avalanche gain, were plotted against 1000/T, where T is the temperature. The temperature dependence of the dark current was modelled using current expressions $I_1 = Aexp\,[(-E_g(T)/2KT)]$ and $I_2 = Bexp\,[(-E_g(T)/KT)]$ where k is Boltzmann's constant, A and B are adjustable constants, and $E_g(T)$ is the bandgap of InAs as a function of temperature [15]. Since the intrinsic carrier concentration is given by $n_i \infty exp\,[(-E_g(T)/2KT)]$, I_1 and I_2 are proportional to n_i and n_i^2 respectively. Both I_1 and I_2 were used to fit the total leakage current across the range $T = 77$ K to 290 K. However, we were unable to achieve satisfactory fit using a single expression from I_1 or I_2.

Further analysis of the dark current was carried out by separating the total leakage current into two components, J_{bulk} the bulk leakage current density (A/cm^2) and J_{surf} the surface current per unit length (A/cm) across the range of applied bias from 0 to 15 V [16]. The dark currents at a fixed voltage for photodiodes with different radii were fitted with the equation $I(T) = \pi r^2 J_{bulk}(T) + 2\pi r J_{surf}(T)$, where r is the radius of the diode [16]. The measured I-V data from diodes with radii of 30μm to 205μm at temperatures from 77 K to 290 K were used as input parameters into an algorithm that searches for the best combination of the $J_{bulk}(T)$ and $J_{surf}(T)$ to

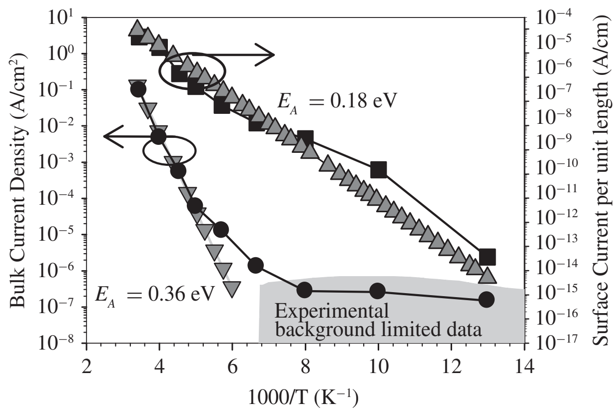

Fig. 2. Comparison between area normalized bulk current J_{bulk} (•) and perimeter normalized surface current J_{surf} (■) with modeled components proportional to n_i^2 (▼) and n_i (▲).

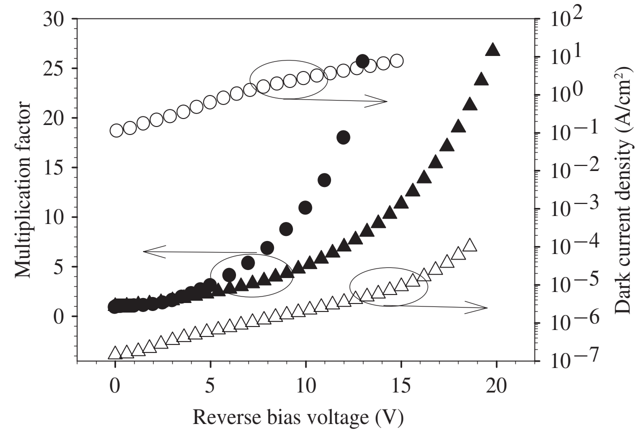

Fig. 3. Avalanche gains at 290 K (•) and 77 K (▲) with dark current densities at 290 K (o) and 77 K (△).

fit the measured $I(T)$. J_{bulk} and J_{surf} at 0.3 V were then plotted against $1000/T$ in figure 2. It is clear that J_{bulk} is well modelled by I_2 for the temperatures between 200 K and 290 K whereas J_{surf} can be fitted by I_1 for the entire temperature range measured. Therefore, J_{bulk} is proportional to n_i^2 while J_{surf} is well described by n_i. The activation energies for J_{bulk} of 0.36 eV and J_{surf} of 0.18 eV were calculated using the Arrhenius equation $J = Cexp[(-E_A/K_T)]$, where C is a constant and E_A is the bulk (or surface) activation energy.

Figure 3 shows the avalanche gains and the dark current densities of the InAs APDs at 290 K and 77 K. A predominantly electron injection profile was obtained by focusing a 633 nm laser onto the p^+−layer. The position of the laser spot was optimised to obtain the maximum multiplication. However there was a small amount of unintentional hole injection through absorption at the mesa side walls. Despite the contamination of hole injection which decreases the avalanche gain, the InAs APD can provide a useful gain of 25 at 13 V and 19.5 V, at 290 K and 77 K respectively. The Responsivity of the InAs photodiode at 0.3 V (unity gain) is approximately 0.25 A/W. The measurement was also checked using 3 different incident light powers ranging between 10μW and 100μW to ensure that there is no heating effect which can cause the avalanche gain to vary.

III. Discussion

With our improved growth, fabrication and passivation techniques, the reverse leakage current of the InAs APDs has been well suppressed. In the reverse bias, tunnelling current was not observed at biases below 15 V at all temperatures due to the low unintentional background doping of $\sim 7\times10^{14}$cm^{-3} and hence low peak electric field. The total leakage current can be modelled by both bulk diffusion and surface generation-recombination currents. The InAs APDs do not show any avalanche breakdown across the entire temperature range measured. This is due to the single carrier multiplication characteristic in InAs APD, which leads to an exponentially rising avalanche gain rather than an abrupt avalanche breakdown. In general the gain, M, is given by $M = \exp(\alpha w)$ and $M = (1\text{-}\alpha w)^{-1}$ for the case of $\beta = 0$ and $\alpha = \beta$ respectively where α is the electron ionization coefficient and β is the hole ionization coefficient. Assuming that electrons are injected to initiate the multiplication process one will observe exponentially rising if the ionization process is only caused by electrons in the case of $\beta = 0$ and when α is only weakly dependent on voltage as has been observed in HgCdTe APDs and InAs APDs. In the case of double carrier ionization such as when $\alpha = \beta$, the breakdown is abrupt as both α and β increases rapidly with bias leading to a dramatic increase in the gain with bias as observed in most of the III-V semiconductors such as GaAs and InP.

Figure 2 shows that the bulk component was proportional to n_i^2 for temperatures above 200 K, clearly indicating that J_{bulk} is dominated by the diffusion of carriers from the cladding layers. The activation energy of this component at 200-290 K was determined to be 0.36 eV, a value very close to E_g. It is worth noting that the J_{bulk} saturates at temperatures below 125 K while the J_{surf} continues to decrease with decreasing temperature. Closer inspection of the forward I-V below 125 K showed that this saturated J_{bulk} is due to the background-induced photocurrent owing to insufficient shielding. On the other hand, J_{surf} is directly proportional to n_i for the entire temperature range reported indicating that the surface current is due to generation and recombination at the surface. The calculated $E_A = 0.18$ eV, which is one-half of the bandgap energy, indicates that there are energy states or energy traps near the mid-bandgap energy level which are acting as generation and recombination centres along the etched mesa surface [17].

To estimate the significance of J_{bulk} and J_{surf} in devices with different dimensions, the bulk leakage currents and surface leakage currents for a large area 2 mm-diameter device and a small $25\times25\mu$m^2 device were modelled using I_1 and I_2 in the absence of background induced photocurrent. The large area photodetector would be of interest for light detection and ranging (LIDAR) and gas sensing purposes while the small $25\times25\mu$m^2 device corresponds to a typical pixel dimension in imaging focal plane arrays. From Figure 4, it can be seen that in the 2 mm-diameter device, the bulk

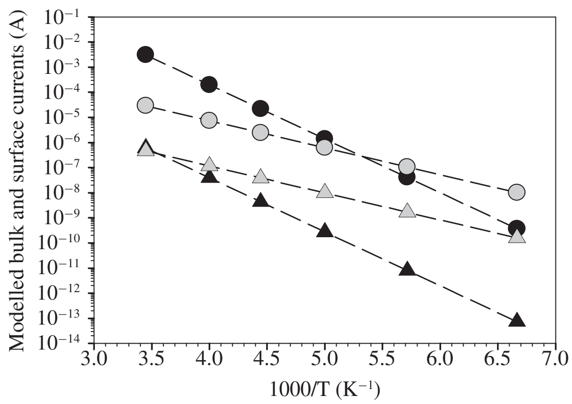

Fig. 4. Modeled bulk (black) and surface (grey) leakage currents of a 2 mm-diameter device (●, ●) and a 25 × 25 μm^2 pixel (▲, ▲) in the absence of background-induced photocurrent from 150 K to 290 K.

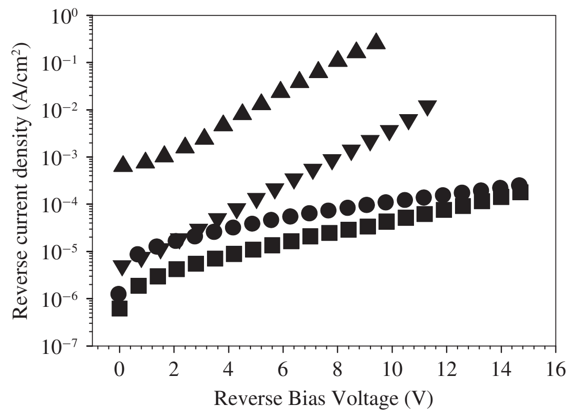

Fig. 5. Reverse dark current densities reported by Reine et al. ($\lambda_c = 4.06$ μm at 160 K) [20](▼) and Perrais et al. ($\lambda_c = 5$ μm at 77 K) [21] (▲) for planar MWIR HgCdTe APDs, compared with the result reported here for an InAs APD (●) and the extracted InAs APD purely bulk current density (■) at 150 K.

leakage current dominates over the surface leakage current at temperatures above 200 K. However, surface leakage current is more significant for a small pixel indicating that more effort is needed to reduce the surface current component if the InAs APD is targeted for focal plane arrays applications.

The dynamic resistance-area product of an APD is important when the APD is interfaced with other circuitry in a system. For instance, most of the commercially available readout integrated circuits (ROICs) for focal plane arrays require a minimum $R_D A$ of 1 kΩ-cm^2. The $R_d A$ of an APD is mainly dependent on the rate of change of dark current with respect to bias voltage. From figure 1, it was shown that the total dark currents increased gradually with increasing reverse bias voltage at each temperature. From 0.1 V to 12 V, the $R_D A$ of the InAs APDs was calculated to be between 3.7 kΩ-cm^2 and 1.1 kΩ-cm^2 at 200 K. It can be estimated, from figure 3, that the avalanche multiplication factor at 200 K is between 7 (77 K) and 18 (290 K) at a bias voltage of 12 V. Therefore, the ROICs minimum $R_D A$ requirement can be satisfied by operating the InAs APDs with useful avalanche gain at temperatures which can be achieved by thermoelectric coolers. The temperature dependence of photomultiplication in InAs APDs, hence the temperature dependence of ionization coefficient is an on-going work. This would be a valuable complementary study to the temperature dependence of leakage current reported in this work since together they will enable designers to determine the extent of cooling necessary for InAs APDs to operate in a particular application.

The temperature dependent dark current and avalanche gain characteristics presented here, show that lowering the operating temperature of these InAs APDs to 77 K can reduce the leakage current substantially, however this is accompanied by an undesirable reduction in the avalanche gain at a given voltage [18], as evident in figure 3. At 77 K, although the bulk diffusion and surface generation current components were suppressed at low bias voltages, the total leakage current was dominated by the band-to-band tunnelling above 15 V. However, avalanche multiplication factors as high as 22 can still be obtained at 18.6 V when a dark current density of 10^{-4} A/cm^2 was assumed to be the maximum acceptable value. The peak electric field was calculated to be ~60 kV/cm at 15 V [18]. To further reduce the tunnelling current, lower $i-$layer background doping is necessary to reduce the peak electric field. A lower background doping will also yield wider depletion widths and therefore higher avalanche multiplication factor at a given bias voltage [19].

Figure 5 compares the dark current densities calculated for the InAs APDs reported here at 150 K with the mid-wave infrared (MWIR) HgCdTe APDs from Reine *et al.* at 160 K [20] and Perrais *et al.* at 150 K [21]. These APDs have cut-off wavelengths of $\lambda_c = 4.06\mu$m and $\lambda_c = 5\mu$m at temperatures of 160 K and 77 K respectively. To facilitate the comparison, the current densities for all the APDs were calculated using the total leakage currents and the device areas. The areas of the HgCdTe APDs from Reine *et al.* and Perrais *et al.* are 6.25×10^{-4}cm^2 and 1×10^{-6}cm^2 respectively whereas the InAs APD with an area of 9.5×10^{-5}cm^2 is used for this comparison. It is clear that the dark current density of the mesa-etched InAs APD is lower than that from Perrais *et al.* and is comparable to that of a planar MWIR HgCdTe APD from Reine *et al.* at biases below 4 V. At higher biases, the InAs APDs showed significantly lower leakage. Moreover, the pure bulk current density extracted from our result is lower still, indicating that planar InAs APDs, fabricated either by ion implantation or diffusion of dopants, could potentially yield lower dark current by eliminating the surface current component.

IV. Conclusion

SU-8 passivated InAs APDs have been fabricated. The temperature dependence of the I-V characteristics of these InAs APDs have been studied in detail. Relatively low dark current densities are achieved at both 77 K and 290 K with $R_d A = 910$ MΩ-cm^2 at 77 K and $R_d A = 34\Omega$-cm^2 at 290 K at 0.1 V bias. Detailed dark current analysis, separating J_{bulk} and J_{surf} leakage components, revealed that the bulk leakage current in these InAs APDs is carrier-diffusion dominated while the surface leakage current is caused by the mid-gap generation and recombination of carriers. The comparison with other APDs technologies reaffirms the importance and potential of having improved mesa or planar InAs APDs to achieve minimum dark current levels and allow the potential benefits to be exploited fully. An avalanche multiplication factor of 25 was measured at 13 V and 19.5 V at temperatures of 290 K and 77 K respectively. The potential to support infrared imaging was demonstrated by the InAs APDs providing avalanche gain up to 22 at 77 K, while operating within an upper limit dark current density specification of 10^{-4} A/cm^2.

REFERENCES

[1] I. Baker, S. Duncan, and J. Copley, "A low-noise laser-gated imaging system for long-range target identification," *Proc. SPIE: Infr. Technol. Appl. XXX*, vol. 5406, pp. 133–144, Sep. 2004.

[2] A. Krier, H. H. Gao, and Y. Mao, "A room temperature photovoltaic detector for the mid-infrared (1.8–3.4 μm) wavelength region," *Semicond. Sci. Technol.*, vol. 13, no. 8, pp. 950–956, May 1998.

[3] M. Achour, "Free-space optics wavelength selection: 10 μm versus shorter wavelengths," *Proc. SPIE: Free-Space Laser Commun. Act. Laser Illuminat. III*, vol. 5160, pp. 234–246, Jan. 2004.

[4] H. H. Gao, A. Krier, V. Sherstnev, and Y. Yakovlev, "InAsSb/InAsSbP light emitting diodes for the detection of CO and CO_2 at room temperature," *J. Phys. D: Appl. Phys.*, vol. 32, no. 15, pp. 1768–1772, 1999.

[5] R. J. McIntyre, "Multiplication noise in uniform avalanche diodes," *IEEE Trans. Electron Dev.*, vol. 13, no. 1, pp. 164–168, Jan. 1966.

[6] J. D. Beck, C. Wan, M. Kinch, J. Robinson, P. Mitra, R. Scritchfield, F. Ma, and J. Campbell, "The HgCdTe electron avalanche photodiode," *Proc. SPIE: Infr. Detector Mater. Dev.*, vol. 5564, pp. 44–53, Oct. 2004.

[7] A. Rogalski, "HgCdTe infrared detector material: History, status and outlook," *Rep. Prog. Phys.*, vol. 68, no. 10, pp. 2267–2336, 2005.

[8] J. M. Dell, J. Antoszewski, M. H. Rais, C. Musca, J. K. White, B. D. Nener, and L. Faraone, "HgCdTe mid-wavelength IR photovoltaic detectors fabricated using plasma induced junction technology," *J. Electron. Mater.*, vol. 29, no. 6, pp. 841–848, Jun. 2000.

[9] A. R. J. Marshall, C. H. Tan, M. J. Steer, and J. P. R. David, "Electron dominated impact ionization and avalanche gain characteristics in InAs photodiodes," *Appl. Phys. Lett.*, vol. 93, no. 11, pp. 111107-1–111107-3, Sep. 2008.

[10] A. R. J. Marshall, C. H. Tan, M. J. Steer, and J. P. R. David, "Extremely low excess noise in InAs electron avalanche photodiodes," *IEEE Photon. Technol. Lett.*, vol. 21, no. 13, pp. 866–868, Jul. 2009.

[11] A. R. J. Marshall, C. H. Tan, J. P. R. David, J. S. Ng, and M. Hopkinson, "Fabrication of InAs photodiodes with reduced surface leakage current," *Proc. SPIE: Opt. Mater. Defense Syst. Technol.*, vol. 6740, pp. 67400I-1–67400I-7, Nov. 2007.

[12] R.-M. Lin, S.-F. Tang, S.-C. Lee, C.-H. Kuan, G.-S. Chen, T.-P. Sun, and J.-C. Wu, "Room temperature unpassivated InAs p-i-n photodetectors grown by molecular beam epitaxy," *IEEE Trans. Electron Dev.*, vol. 44, no. 2, pp. 209–213, Feb. 1997.

[13] R.-M. Lin, S.-F. Tang, S.-C. Lee, C.-H. Kuan, "Improvement of current leakage in the InAs photodetector by molecular beam epitaxy," *J. Cryst. Growth*, vols. 227–228, pp. 167–171, Jul. 2001.

[14] H. S. Kim, E. Plis, A. Khoshakhlagh, S. Myers, N. Gautam, Y. D. Sharma, L. R. Dawson, S. Krishna, S. J. Lee, and S. K. Noh, "Performance improvement of InAs/GaSb strained layer superlattice detectors by reducing surface leakage currents with SU-8 passivation," *Appl. Phys. Lett.*, vol. 96, no. 3, pp. 033502-1–033502-3, Jan. 2010.

[15] Z. M. Fang, K. Y. Ma, D. H. Jaw, R. M. Cohen, and G. B. Stringfellow, "Photoluminescence of InSb, InAs, and InAsSb grown by organometallic vapor phase epitaxy," *J. Appl. Phys.*, vol. 67, no. 11, pp. 7034–7039, Jun. 1990.

[16] X. G. Zheng, J. S. Hsu, J. B. Hurst, X. Li, S. Wang, X. Sun, A. L. Holmes, J. C. Campbell, A. S. Huntington, and L. A. Coldren, "Long-wavelength $In_{0.53}Ga_{0.47}As$–$In_{0.52}Al_{0.48}As$ large-area avalanche photodiodes and arrays," *IEEE J. Quantum Electron.*, vol. 40, no. 8, pp. 1068–1073, Aug. 2004.

[17] S. R. Forrest, R. F. Leheny, R. E. Nahory, and M. A. Pollack, "$In_{0.53}Ga_{0.47}As$ photodiodes with dark current limited by generation-recombination and tunneling," *Appl. Phys. Lett.*, vol. 37, no. 3, pp. 322–324, Aug. 1980.

[18] A. R. J. Marshall, P. Vines, P. J. Ker, J. P. R. David, and C. H. Tan, "Avalanche multiplication and excess noise in InAs electron avalanche photodiodes at 77 K," *IEEE J. Quantum Electron.*, vol. 47, no. 6, pp. 858–864, Jun. 2011.

[19] A. R. J. Marshall, J. P. R. David, and C. H. Tan, "Impact ionization in InAs electron avalanche photodiodes," *IEEE Trans. Electron Dev.*, vol. 57, no. 10, pp. 2631–2638, Oct. 2010.

[20] M. B. Reine, J. W. Marciniec, K. K. Wong, T. Parodos, J. D. Mullarkey, P. A. Lamarre, S. P. Tobin, and K. A. Gustavsen, "HgCdTe MWIR back-illuminated electron-initiated avalanche photodiode arrays," *Proc. SPIE: Infr. Photoelectron. Imagers Detect. Dev. II*, vol. 6294, pp. 629403-1–629403-17, Sep. 2006.

[21] G. Perrais, O. Gravrand, J. Baylet, G. Destefanis, and J. Rothman, "Gain and dark current characteristics of planar HgCdTe avalanche photo diodes," *J. Electron. Mater.*, vol. 36, no. 8, pp. 963–970, 2007.

Pin Jern Ker received the B.E. (hons.) degree in electrical and electronic engineering from the University of Tenaga Nasional, Putrajaya, Malaysia, in 2009. He is currently pursuing the Ph.D. degree at the University of Sheffield, Sheffield, U.K.

His current research interests include fabrication and characterization of high performance photodiodes and avalanche photodiodes for mid-infrared applications.

Andrew R. J. Marshall received the M.Eng. (hons.) and Ph.D. degrees in electronic engineering from the University of Sheffield, Sheffield, U.K., in 1999 and 2010, respectively.

He joined Ford Motor Company, London, U.K., in 1999, and Visteon, in 2000, where he was on the design and manufacturing of car instruments and displays until 2004. In 2005, he became a Chartered Engineer. Between 2008 and 2010, he was a Researcher at the University of Sheffield. Currently, he is in the Physics Department, Lancaster University, Lancaster, U.K., where he holds a Royal Academy of Engineering research fellowship. His current research interests include theory, characterization and fabrication of high performance photodiodes, and avalanche photodiodes.

Andrey B. Krysa was received the Graduate degree in quantum electronics from Moscow Engineering Physics Institute, Moscow, Russia, in 1990, and the Ph.D. degree in solid state physics from Lebedev Physical Institute of the Russian Academy of Sciences, Moscow, in 1997.

He joined the Department of Optoelectronics, Lebedev Institute, Moscow, in 1995, as a Research Scientist, and performed research on II–VI compounds. From 1999 to 2000, he was with the Institut für Halbleitertechnik, Rheinisch-Westfälische Technische Hochschule Aachen, Aachen, Germany, researching the problem of ZnSe homoepitaxy and related structures for light-emitting devices. Since joining the Engineering and Physical Sciences Research Council National Center for III–V Technologies, Sheffield, U.K., he has been engaged in research on metalorganic-vapor-phase epitaxy (MOVPE) of the group III arsenides and phosphides and related semiconductors. In Sheffield, he developed a growth technology of quantum cascade lasers entirely based on MOVPE, high performance red-emitting semiconductor disc lasers, laser diodes based on InP quantum dots and other advanced semiconductor structures.

Dr. Krysa was awarded a prestigious Humboldt Research Fellowship in 1999. He is a recipient of the Institute of Engineering Technology Optoelectronics Premium Award in 2008.

John P. R. David (SM'96) received the B.Eng. and Ph.D. degrees in electronic engineering from the University of Sheffield, Sheffield, U.K.

He was with the Central Facility for III–V Semiconductors, Sheffield, from 1985 to 2000, where he was responsible for the characterization activity. From 2000 to 2001, he was with Marconi Optical Components (now Bookham Technologies), Towcester, U.K., before returning to an academic position at the University of Sheffield. He is currently a Professor and the Head of the Department at the Department of Electronic and Electrical Engineering, University of Sheffield. His current research interests include impact ionization and avalanche photodiodes, and III–V material characterization.

Dr. David was the IEEE Lasers and Electro Optics Society Distinguished Lecturer from 2002 to 2004.

Chee Hing Tan (M'95) received the B.Eng. and Ph.D. degrees in electronic engineering from the Department of Electronic and Electrical Engineering, University of Sheffield, Sheffield, U.K., in 1998 and 2002, respectively.

He has been with the Department of Electronic and Electrical Engineering, University of Sheffield, since 2003, where he is currently a Reader. He has extensive experience in characterization and modeling of high speed low noise avalanche photodiodes and phototransistors. His current research interests include single photon avalanche diodes, mid-infrared photodiodes, quantum dot infrared detectors, X-ray detectors and ultrahigh speed avalanche photodiodes and phototransistors.